Direct and valence neutron capture by ^{7}Li

J. E. Lynn and E. T. Jurney
Los Alamos National Laboratory, Los Alamos, New Mexico 87545

S. Raman
Oak Ridge National Laboratory, Oak Ridge, Tennessee 37831
(Received 11 February 1991)

We have measured the cross section for neutron radiative capture by ^{7}Li at thermal neutron energy as 45.4±3.0 mb. We have compared this value, and the available fast-neutron-capture cross-section data on ^{7}Li, with direct- and valence-capture theory. The mechanism of direct capture involving simple neutron-orbital transitions within a potential well can adequately account for the magnitude of the thermal-neutron-capture cross sections and the shape of the fast-neutron-capture cross sections. We recommend that the capture cross sections from the theoretical calculation, instead of those from a recent measurement, be used for nuclear astrophysics calculations. If the fast-neutron-capture data are normalized at 25 keV to the theoretical value, the magnetic-dipole ($M1$) radiation width of the 255-keV p-wave resonance can be deduced. It is in agreement with the value calculated from a valence theory for $M1$ capture, thus lending support for this neutron-capture mechanism as an important one, at least for light nuclei. We also find some evidence from our analysis of the total cross-section data for a possible energy dependence of the potential required to describe the almost pure single-particle s-wave resonances underlying the ^{7}Li cross section.

I. INTRODUCTION

The neutron-capture cross section of ^{7}Li and its relation to the scattering properties of that nucleus are of considerable interest for several reasons: (1) Because the compound system ^{8}Li is a light nucleus with its low-lying states dominated by the $1p_{3/2}$ single-particle (s.p.) configurations, it is a prime candidate for thermal (0.025-eV) neutron capture to be governed by the direct-capture [1,2] mechanism. (2) This mechanism will be unusual in this case because one of the key parameters establishing its magnitude, the thermal-neutron-scattering length, is negative. (3) The apparent absence of s-wave resonances in the cross section up to MeV neutron energies indicates that the direct mechanism for electric-dipole ($E1$) transitions should still be dominant in this higher-energy region and could be tested against the existing data. (4) Radiative decay from the strong p-wave resonance at 255 keV will be dominated by a magnetic-dipole ($M1$) transition, giving an opportunity to test valence models for this class of transitions. (5) The ^{7}Li(n,γ) reaction is a key reaction in the formation of $A \geq 12$ nuclides in the early stages of nucleosynthesis [3].

Indeed, it was the publication of new data [4] on ^{7}Li(n,γ) that prompted this study. These data indicate that the fast-neutron-capture cross section may be more than a factor of 2 lower than that found in earlier measurements [5], thus suggesting reduced feeding of a primordial r process. They also yield a new estimate of the $M1$ capture width of the 255-keV resonance.

This paper is organized as follows. In Sec. II we describe the measurement of the thermal-neutron-capture cross section and show that the direct- (or potential-) capture model can reproduce this cross section reasonably well. A simple extrapolation, using the inverse neutron-velocity relationship ($1/v$), of the measured cross section at thermal energy to neutron energies of 25 keV and greater, gives agreement, within a factor of 2, between the measured and calculated capture cross sections at these energies, suggesting that the direct mechanism operates also for fast neutrons. A more substantive test requires the analysis of the total cross section and elastic-scattering angular-distribution data to determine the s-wave scattering lengths in this energy region, because it is primarily on these quantities that the direct-capture estimate depends. This analysis is described and discussed in Sec. III. A side issue of special interest is that the s-wave cross section has the features of a s.p. resonance in a real potential well, but the parameters of this well must be energy dependent to correctly describe the cross section. Such energy dependence is known to be a requirement of optical-model potentials that give global descriptions of cross-section data in much heavier nuclei [6,7]. The calculation of the neutron-capture cross section for $E1$ transitions over the energy range up to several hundred keV is described in Sec. IV. We show that certainly up to 150 keV, this cross section does indeed behave as $1/v$. This conclusion agrees more nearly with the older data of Imhof *et al.* [5] than with the newer data of Wiescher, Steininger, and Käppeler [4]. We then assume the correctness of the theory and normalize at 25 keV the cross section of Ref. [4] to the calculated value. This procedure enables us to extract the (p-wave) resonance-capture cross section and, hence, the radiation width, which comprises a single $M1$ transition. We outline the theory of $M1$ valence radiation widths in Sec. V and use the well-measured neutron width of the 255-keV resonance to estimate its expected radiation

width. The agreement with measurement is good and helps establish the almost universal importance of the direct and closely related valence mechanisms for both $E1$ and $M1$ transitions in neutron capture by very light nuclei. Our conclusions are summarized in Sec. VI.

II. THERMAL-NEUTRON CAPTURE

We have measured the energies and intensities of the three possible prompt γ rays from the ^{7}Li$(n,\gamma)^8$Li reaction [8]. Gamma rays from a 1.4-g target of Li_2CO_3 (99.994% enriched in ^{7}Li) placed in the internal target facility of the Los Alamos Omega West reactor were viewed by a 25-cm^3 Ge(Li) detector surrounded by a NaI(Tl) Compton-suppression annulus. This facility and data analysis procedures have been described in detail in Ref. [2]. The Cd ratio at the target position is $\sim$1000. A separate run with this target and with a 100.5-mg target of CH_2 was made so that the γ-ray intensities could be related to the accurate value [9] for hydrogen capture, $\sigma_c(^1\text{H})=332\pm1$ mb. The energy calibration for the ^{7}Li capture γ rays was established by the 1261.76±0.03-keV γ ray from capture by ^{12}C (graphite target holder) and by the 2223.25±0.02-keV γ ray from hydrogen capture resulting from the 18-mg water content of the slightly hygroscopic Li_2CO_3. This target material also contained trace amounts (ppm in parentheses) of Na(80), Al(10), Mg(150), Si(150), K(80), Ca(1300), Ni(20), and Ag(6), all of which are expected in varying degrees, and Hg(200), which was not expected. The above impurities, however, did not pose a serious problem in the measurements.

Three γ rays in ^{8}Li could be identified (see Fig. 1) following neutron capture by ^{7}Li. These are tabulated in Table I. Although the absolute intensities of the 981- and 1052-keV γ rays that form a cascade can be stated only to an accuracy of $\sim$10%, their intensities relative to each other are equal to within $\sim$1%. The radiative capture cross section was obtained by summing the partial cross sections. The known sources of uncertainty produce an uncertainty of 1.5 mb in the total cross section, but this value was doubled to account for all unknown sources. The final result, $\sigma=45.4\pm3.0$ mb, together with previously reported values is given in Table II.

The data required to estimate the direct-capture cross section are the (spin-dependent) neutron-scattering lengths and the (d,p) spectroscopic factors for the s.p. neutron components of the final states. In the case of the ^{7}Li target nucleus (spin and parity $I^\pi=\frac{3}{2}^-$), both sets of data are known. The coherent neutron-scattering length of ^{7}Li is -2.22 ± 0.02 fm, and the spin-dependent components are $a_+=-3.63\pm0.05$ fm ($J=2$) and $a_-=+0.87\pm0.07$ fm ($J=1$). These values are from Christiansen filter and transmission measurements [10]. The spectroscopic factor θ_f^2 of the $1p_{3/2}$ neutron configuration in the ground state of ^{8}Li is 0.87 and that of the 0.98-MeV state is 0.48 (Ref. [11]).

The detailed theory and methods for calculating the direct-capture cross sections from such data have been dealt with extensively in Refs. [2] and [12–15]. The essence of the method is to calculate the matrix element between the s.p. component of the initial scattering wave function and that of the final-state wave function. Most of the contribution to the radial $E1$ overlap integral comes from the channel region of configuration space (and hence is often referred [1] to loosely as "channel capture"), where the magnitude of the initial wave function is governed by the scattering length (which also yields the total and coherent-scattering cross sections) and that of the final state by its binding energy and spectroscopic factor. The radial overlap integrals are usually generated from an optical-model calculation for the initial wave function and a real-potential-well model for the final state. Global potentials based on the Woods-Saxon form are usually taken as the starting point, but the potential depth, in particular, is often varied so as to give the correct binding energy for the final state and the correct scattering length for the initial (capture) state. Sometimes the results of this variation lead to considerable distortion of the potential parameters from their global values. In this case, a correction to the valence radiation width can be made (using the imaginary component of the radial integral), yielding an estimate of the average

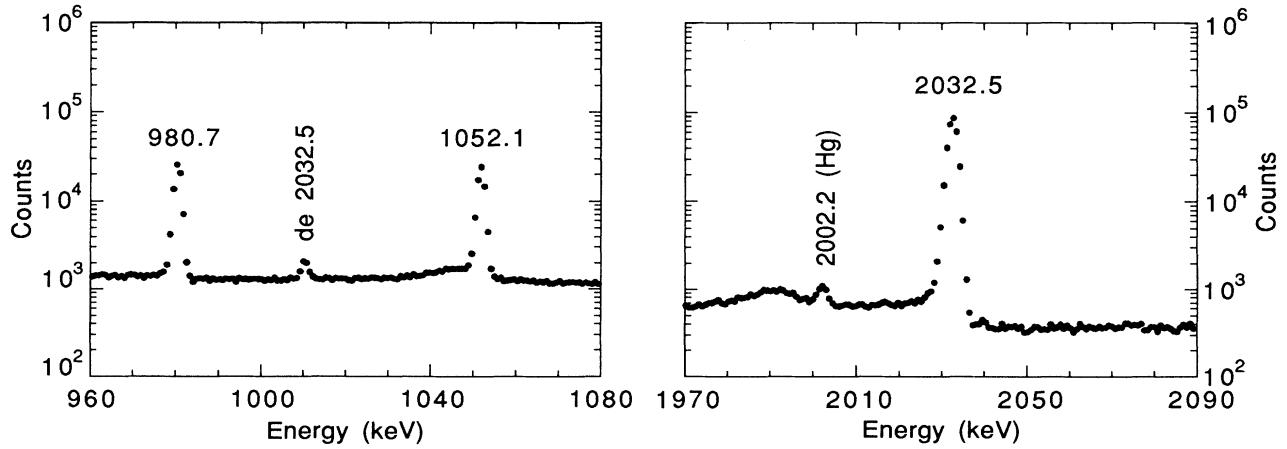

FIG. 1. Selected portions of the γ-ray spectrum from the ^{7}Li$(n,\gamma)^8$Li reaction with thermal neutrons.

TABLE I. Measured energies (E) and intensities (I) of γ rays from thermal neutron capture by ^{7}Li.

This work E_γ (keV)[c]	This work I_γ (mb)	This work I_γ (γ/100n)	Jarczyk *et al.*[a] I_γ (γ/100n)	Orphan *et al.*[b] I_γ (γ/100n)
980.6±0.2	4.82±0.50	10.6±1.0	30	9.8
1052.0±0.2	4.80±0.50	10.6±1.0	20	4.9
2032.5±0.3	40.56±1.0	89.4±1.0	80	89.3

[a]L. Jarczyk, J. Lang, R. Müller, and W. Wölfli, Helv. Phys. Acta **34**, 483 (1961).
[b]V. J. Orphan, N. C. Rasmussen, and T. L. Harper, Gulf General Atomic Report GA-10248 (1970). The results obtained with a natural target have been renormalized to take into account the abundance of ^{7}Li in Li.
[c]Not corrected for recoil.

valence radiation width in local levels that may distort the local scattering length from its optical-model value.

In the current case there are clearly no local levels in the usual sense to be considered. Hence all our calculations have been made using real-potential models. There is, of course, some uncertainty in the calculation of the capture cross section stemming from the choice of potential parameters. By studying a range of reasonable choices of the potential, we estimate this uncertainty as being ~10%. For example, for the Woods-Saxon potential form,

$$\mathcal{V}(r)=\frac{\mathcal{V}_0}{1+\exp[(r-R)/d]}+\frac{(\boldsymbol{l}\cdot\boldsymbol{\sigma})K\mathcal{V}_0\exp[(r-R)/d]}{rd\{1+\exp[(r-R)/d]\}^2}, \quad (1)$$

where K is the spin-orbit coupling constant (chosen numerically to be 0.0043 b) between the neutron spin σ and orbital angular momentum l, the choice of $d=0.5$ fm, $R=2.5$ fm, and $\mathcal{V}_0=-60.3$ MeV gives a thermal-neutron scattering length of -3.6 fm (the experimental datum for the initial $J=2$ state) and a capture cross section of 26 mb (for the transition from the $J=2$ initial state to the ground state). For the parameter choice $d=0.56$ fm, $R=2.68$ fm, and $\mathcal{V}_0=-51.3$ MeV, which gives the same scattering length, the capture cross section is 29 mb. (These cross-section estimates contain the spin-angle component of the matrix element, the final-state spectroscopic factor, and the statistical spin-weighting factor of the initial state.) In the case of the $J=1$ initial state, the choice of diffuseness and radius parameters, $d=0.5$ fm, $R=2.5$ fm, requires a potential depth of 50.5 MeV to reproduce the scattering length of 0.9 fm, and the capture cross section to the ground state is then 9.8 mb. The total cross section for transitions to the ground state is thus 36 mb.

With a similar choice of parameters, the cross sections to the first-excited state are 0.9 mb (for $J=2$) and 2.0 mb (for $J=1$), giving a total of 2.9 mb for the 1052-keV transition. The calculated branching ratio $I(1052\gamma)/I(2033\gamma)=0.08$ agrees reasonably well with the experimental ratio of 0.12±0.01. The total capture cross section is thus 39 mb. The uncertainty in this value due to the uncertainty in the spectroscopic factors alone is ~20%. The calculated value of 39 mb thus agrees well with the experimental value 45.4±3.0 mb if the above uncertainty is taken into account. We conclude therefore that the direct-capture theory provides a sound explanation of the thermal-neutron-capture data.

TABLE II. Thermal-neutron-capture cross section $\sigma(n,\gamma)$ of ^{7}Li.

$\sigma(n,\gamma)$ (mb)	Reference
33±5	Hughes *et al.*[a]
44±10	Koltypin and Morozov[b]
40±8	Imhof *et al.* (Ref. [5])
40±12	Jarczyk *et al.* (see Table I)
45.4±3.0	this work

[a]D. J. Hughes, D. Hall, C. Eggler, and E. Goldfarb, Phys. Rev. **72**, 646 (1947).
[b]E. A. Koltypin and V. M. Morozov, Dokl. Akad. Nauk SSSR **111**, 331 (1956) [Sov. Phys. (Dokl.) **1**, 655 (1956)].

III. TOTAL CROSS-SECTION AND SCATTERING DATA

The total cross section of ^{7}Li up to several MeV neutron energy shows a few broad resonance features, none of which have characteristic s-wave properties, and yet the values of the thermal-neutron-scattering lengths imply that there is strong s-wave resonance strength in the epithermal region. The absence of sharp fine-structure resonances suggests that this s-wave strength resides in the form of a s.p. resonance which is almost completely undamped into narrow compound-nuclear resonances; such a resonance at a few hundred keV or higher will appear in the cross section as only a broad background feature.

An estimate can be made of the expected reduced neutron width (as defined in $\mathcal{R}$-matrix theory [16,17]) of such an s.p. resonance in a potential well that could represent a nucleus the size of ^{7}Li. We use a Woods-Saxon form [Eq. (1)] with the potential cutoff at a radius defined by $r_c=R+7d$. This radius will also serve as the channel radius a_c. We then determine the properties of an $\mathcal{R}$-matrix state defined with a boundary condition $B_c=0$ at the channel radius. We can fix the eigenvalue E_λ at a given value (say, 1 MeV) and determine the correspond-

ing potential parameters, or we can fix the potential parameters and determine the eigenvalue. In either case, the reduced width amplitude γ_λ is determined from the value of the wave function $u(r)$ at the channel radius:

$$\gamma_\lambda=(\hbar^2/2ma_c)^{1/2}u(a_c)\ . \tag{2}$$

Here m is the reduced mass of the neutron-target system. For potential wells with radius $R=2.5$ fm and diffuseness $d=0.5$ fm, the eigenvalue (of the $2s_{1/2}$ state) can be fixed at about 1 MeV with potential depths of the order of 60 MeV. Such an eigenstate has a reduced width γ_λ^2 of 1.14 MeV (channel radius 6.0 fm). Broader, more diffuse wells give reduced widths not much different from this value. For example, with $R=2.82$ fm, $d=0.62$ fm, and a well depth of 45.1 MeV, the reduced width is 0.83 MeV for a channel radius of 7.16 fm.

From the thermal-neutron-scattering length, we can now estimate the approximate location of the s.p. eigenstate. The scattering length at low energy E is related to the eigenvalue parameters by

$$a_{sc}=a_c[1-\gamma_\lambda^2/(E_\lambda-E)-\mathcal{R}_\infty]\ , \tag{3}$$

where $\mathcal{R}_\infty$ is the contribution to the $\mathcal{R}$ function from much more distant levels. If, for simplicity, we ignore $\mathcal{R}_\infty$—an assumption that is valid at the level of approximation we are dealing with here—then, using the reduced width from the deeper (60-MeV) potential above, we find $E_\lambda=0.71$ MeV for the $J=2$ state and $E_\lambda=1.35$ MeV for the $J=1$ state. We can now use these eigenvalues as starting values for a least-squares fit of the total cross section and elastic-scattering angular distributions to an $\mathcal{R}$-matrix representation. (For the 60-MeV potential well, the value of $\mathcal{R}_\infty$ is actually 0.39, which, if included in the analysis, has the effect of raising the eigenvalue E_λ by about 0.2 MeV. The parameter $\mathcal{R}_\infty$ is, in fact, included in the detailed analyses presented below.)

A very comprehensive $\mathcal{R}$-matrix fit to these data up to 8 MeV has already been made by Knox and Lane [18]. In their analysis, the $J^\pi=1^-$ state is at 5.23 MeV (in the laboratory neutron energy scale) with a reduced width of 0.34 MeV. This combination, however, is not adequate for properly explaining the thermal-neutron-scattering length. Moreover, their $J^\pi=2^-$ ($l=0$) state appears at 2.90 MeV neutron energy with a reduced width of 5 MeV (for a channel radius of 4.3 fm); that width is about 3 times as large as the full s.p. state width (allowing for the different channel radius employed in the analysis of Ref. [18]). There is also a second 2^- state at 6.60 MeV with a reduced width of 1.2 MeV. Together, then, these two states have reduced widths summing to some 4 times the full s.p. width expected in this energy region. (This point is recognized in Ref. [18], where it is remarked that these reduced widths exceed the Wigner limit.) The parameters of Ref. [18], therefore, appear unphysical in the context of properly explaining the data in the low-energy region.

This situation has been adjusted in a later, mainly theoretical, analysis by Knox, Resler, and Lane [19] in which the properties of the $\mathcal{R}$-matrix states have been calculated from the shell model and only a few adjustments have been made to accommodate key experimental data. The s-wave states are amongst those thus adjusted, and their parameters are closer to the s.p.-state values that we expect from the above considerations. However, Ref. [19] is aimed at a global understanding of the cross sections over an excitation energy range of almost 10 MeV, and it is not clear that their representation of the s-wave cross section up to about 0.5 MeV is sufficiently precise for our purposes.

We have therefore reanalyzed the energy range up to about 1.5 MeV. A fit to the total cross-section data [20] in the 100–400-keV region is shown in Fig. 2. The $\mathcal{R}$-matrix parameters are listed in Table III. A remark is required here about the value of the p-wave distant-level $\mathcal{R}$ function $\mathcal{R}_\infty$ ($l=1$). With $R=2.5$ fm and $d=0.6$ fm, $\mathcal{V}_0$ is required to be -38.8 MeV to bind a s.p. state at -2.03 MeV. Although the $\mathcal{R}$-matrix eigenvalues for this potential do include a level close to this energy and the next level is at 13 MeV, the p-wave scattering cross section calculated for this potential shows a broad resonancelike effect at about 1 MeV neutron energy. This effect has to be classed as an "echo resonance" in the p-wave scattering [21]. There is no evidence for such a feature in the data; therefore, a much different potential well depth must be chosen to give some realistic representation of the p-wave potential scattering, and this has been studied for a range of well depths. For example, with a well depth of 46 MeV, a total p-wave scattering cross section of 0.7 b at 1 MeV is found. Clearly, this value can be accommodated within the bounds of the data (see Fig. 4), and we have therefore used a distant-level $\mathcal{R}$ function, based on such a cross-section calculation, as a fixed parameter in the fitting. At higher energies, some energy variation is required in the distant-level $\mathcal{R}$ function; therefore, we have employed the approximate relation

$$\mathcal{R}_\infty\approx A+B(E-E_B)\ , \tag{4}$$

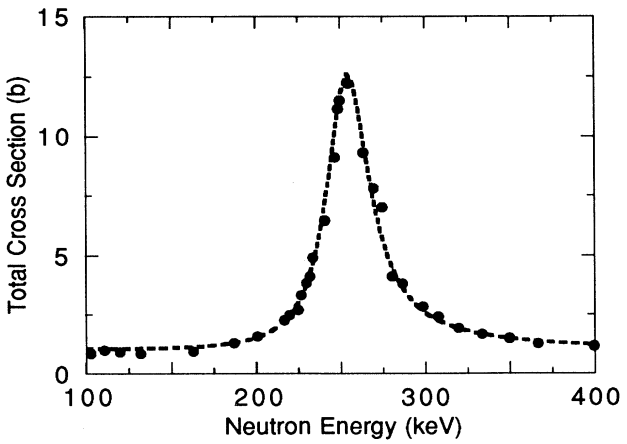

FIG. 2. Total cross section of ^{7}Li from 100 to 400 keV. The data are from Ref. [20]. The parameters for the fitted curve are given in Table III.

TABLE III. $\mathcal{R}$-matrix parameters for the 90–400-keV neutron energy range. The channel radius is 6.0 fm, and the boundary condition is calculated as the $\mathcal{R}$-matrix shift factor at 1 MeV.

J^π	l	$\mathcal{R}_\infty$	E_λ (MeV)	γ_λ (MeV$^{1/2}$)
1^-	0	0.2	1.74	1.068
2^-	0	0.2	0.81	1.068
3^+	1	0.3	0.2145	0.371

where E_B is the energy at which the boundary condition is calculated (see Table IV). For representing the scattering cross section corresponding to the 46-MeV deep potential, values of $A=0.011$ and $B=0.11$ MeV^{-1} are quite reasonable. However, when applied to the analysis of the experimental data, these parameters give too high a cross section at 0.4 MeV. The parameters $A=0.38$ and $B=0.11$ MeV^{-1} (equivalent to $\mathcal{R}_\infty=0.3$ at 0.25 MeV) give a much improved fit to the experimental data. These parameters give a p-wave potential scattering cross section similar to that from a 56-MeV deep well.

In Figs. 3(a)–3(d) we show a selection of fits to the elastic-scattering angular-distribution data [22]. These are normalized to the angle-integrated cross sections, but the normalized factors do not differ by more than 10% from unity; otherwise, the same parameters are used as in Fig. 2 based on Table III. There are some discrepancies between the fits and the data at extreme back angles for the subresonance and sub-centrifugal-barrier neutron energies of 185 keV [Fig. 3(a)] and 215 keV [Fig. 3(b)]. The cross sections are small here and therefore carry larger uncertainties than for the data at more forward angles. At back angles, it is also possible that small deficiencies in the $\mathcal{R}$-matrix treatment of the p-wave contribution to the scattering amplitude could be showing up as a result of destructive interference with the s-wave amplitude. Otherwise, the fits are good, thus establishing that the ratio between p- and s-wave components in the cross section generated from these parameters is reasonable.

At higher neutron energies, around 1.3 MeV, the cross section is dominated by another large p-wave resonance, which is identified in Ref. [18] as a $J^\pi=1^+$ resonance. Both channel spins $s=1$ and 2 can contribute to the formation of this resonance, and the reduced width amplitudes are given (in Ref. [18]) the values 0.5 and 1.0 MeV$^{1/2}$ (channel radius 4.3 fm), respectively. Our fits, which include the effect of the next obvious (p-wave) resonance at about 2.5 MeV, are shown in Fig. 4 for the total cross section and in Fig. 5 for three angular distributions. The deviation of the fitted curve in Fig. 4 above about 1.5 MeV is explained in Ref. [18] by the inclusion of $J^\pi=0^+$ ($l=1$) and 0^- ($l=2$) levels, but here we do not seek to establish a detailed fit to these much higher energies [see also Fig. 5(c)] and do not include them in the analysis. The $\mathcal{R}$-matrix parameters used in the fit are shown in Table IV. The reduced widths for the two alternative channel spins are denoted by s ($=1$) and s' ($=2$). The conclusion from this analysis is that the s-wave $\mathcal{R}$-matrix states we have postulated here (on the basis of the expected properties of s.p. states in a realistic well and the well-known scattering properties of ^{7}Li at thermal-neutron energy) are adequate to explain the s-wave scattering up to at least 1 MeV.

From the s-wave parameters of Table IV, we now calculate the scattering cross section separately for the two spin states up to several hundred keV and seek to find a set of potential-well parameters that will reproduce them. This set can then be used to compute the potential-capture cross section. In fact, we have been unable to find a single potential that represents the scattering cross section over this range. One or more parameters of the potential well have to be varied with neutron energy. A typical calculation is shown in Table V for the $J^\pi=2^-$ component. Here the potential well is assumed to have the fixed radius $R=2.5$ fm and the diffuseness parameter $d=0.5$ fm, and the potential depth is varied. The quantity σ_{fit} is the $J^\pi=2^-$ cross section (divided by the spin-weighting factor g_J) that is calculated from the $\mathcal{R}$-matrix parameters of Table III, and σ_{pot} is that calculated from the potential. The energy E is the neutron energy in the laboratory frame.

It is apparent that there is a significant dependence of the potential depth on the neutron energy. This dependence is by no means unambiguously determined; it can be reduced or otherwise changed by introducing variation of the other Woods-Saxon potential parameters. Nevertheless, it does appear to be consistent with the sense of the energy variation due to the Fermi-surface anomaly from a nonlocal optical potential as discussed extensively for much heavier nuclei in, for example, Ref. [7]. A similar energy dependence is found for the $J^\pi=1^-$ component of the cross section.

TABLE IV. $\mathcal{R}$-matrix parameters for the upper neutron energy range. The channel radius is 6.0 fm, and the boundary condition is calculated as the $\mathcal{R}$-matrix shift factor at 1 MeV. The channel spins are denoted by s ($=1$) and s' ($=2$).

J^π	l	$\mathcal{R}_\infty$	E_λ (MeV)	$\gamma_{\lambda s}$ (MeV$^{1/2}$)	$\gamma_{\lambda s'}$ (MeV$^{1/2}$)
1^-	0	0.2	1.74	1.068	
2^-	0	0.2	0.81		1.068
1^+	1	0.3	1.30	0.565	0.713
2^+	1	0.3	2.50	0.000	0.750
3^+	1	0.3	0.2145		0.371

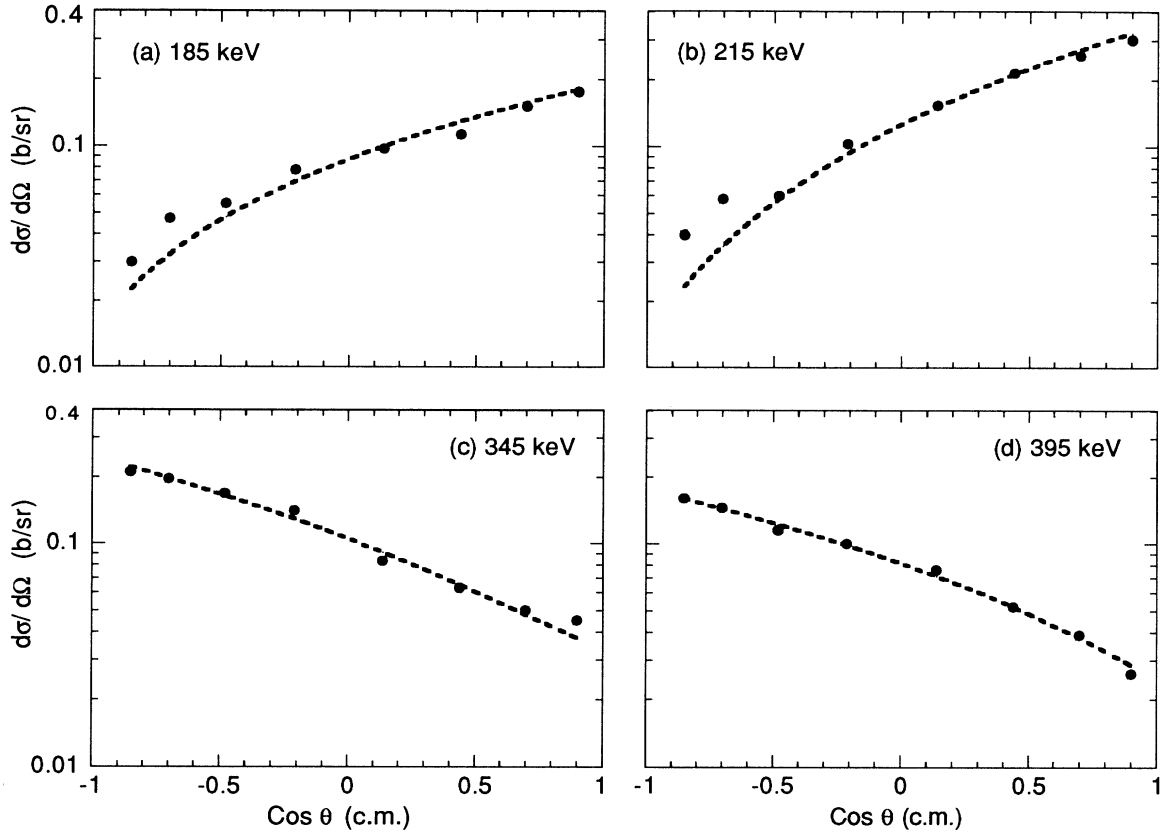

FIG. 3. Angular distribution of elastically scattered neutrons at different neutron energies. The data are from Ref. [22]. The respective curves employ the parameters of Table III.

IV. $E1$ CAPTURE FOR FAST NEUTRONS

The ^{7}Li$(n,\gamma)^8$Li cross sections for fast neutrons, which are difficult to measure because they are in the 10–100-μb range, have been measured by Imhof *et al.* [5] and by Wiescher, Steininger, and Käppeler [4]. In both cases, the incident neutrons were generated by the ^{7}Li$(p,n)^7$Be reaction. Imhof *et al.* [5] employed a natural LiI crystal as a target and detected the capture reaction by observing the β decay of ^{8}Li in their crystal. The capture cross sections in the 40–1000-keV range (and also at thermal) were obtained relative to the known cross sections for the ^{6}Li$(n,t)^4$He and ^{127}I$(n,\gamma)^{128}$I reactions, which also took place in the same crystal. For measurements at 25 keV neutron energy, Wiescher, Steininger, and Käppeler [4] used a LiF sample and an ionization chamber for the detection of the β-delayed α activity of ^{8}Be resulting from ^{8}Li decay. For measurements in the 25–420-keV region, these authors used a Li-glass detector which served both as a target and as a detector of the β activity of ^{8}Li plus the α activity of ^{8}Be. The ^{7}Li$(n,\gamma)^8$Li cross sections were obtained relative to the known ^{197}Au$(n,\gamma)^{198}$Au cross sections. Wiescher, Steininger, and Käppeler [4] pointed out that their ^{7}Li$(n,\gamma)^8$Li cross sections were significantly smaller (on average by a factor of 2–3) than the Imhof *et al.* [5] values.

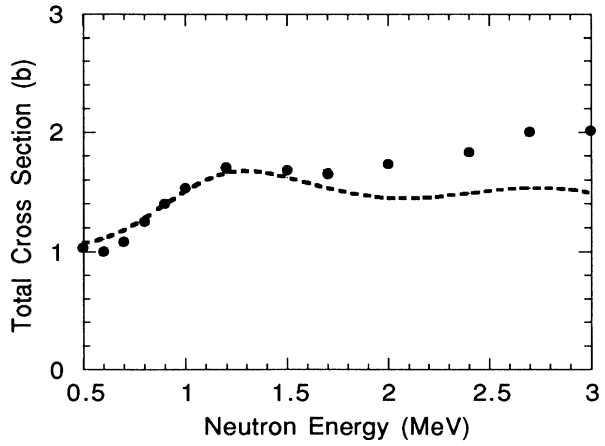

FIG. 4. Total cross section of ^{7}Li from 0.5 to 3.0 MeV. The data are from Ref. [20]. The parameters for the fitted curve are given in Table IV.

We calculate the $E1$ potential-capture cross section with the potentials that reproduce the s-wave scattering cross sections. The result is shown in Fig. 6. Concerning the contributions to the $E1$ capture cross section, al-

though the $J=1$ scattering cross section is small, this spin component of the capture cross section is commensurate with that of $J=2$. Indeed, at 400 keV, the two components are almost exactly equal, whereas at thermal the $J=1$ component is only 60% of the other. At 400 keV the branching ratio $I(1052\gamma)/I(2033\gamma)$ is 0.13, almost exactly equal to the thermal value of 0.12 ± 0.01. Also at 400 keV, most of the cross section to the first-excited state (80%) comes from the $J=1$ initial state.

We note that the change in calculated cross section from thermal to 25 keV is almost exactly proportional to $1/v$. The data of Ref. [5] lie some 20% above this extrapolation, whereas those of Ref. [4] are a factor of 2 below. Both sets of data follow the $1/v$ relation approximately from about 25 to over 100 keV. We believe that even if the basic direct-capture mechanism is not the only factor governing the $E1$ capture cross section over the range from zero to 25 keV—a range that is small compared with the level spacings in the ^{8}Li system—no mechanism could cause the kind of deviation from $1/v$ that is implied by the data of Ref. [4]. A direct-capture model has been proposed [4] that does agree with these data, but the parameters give rise to a scattering cross section that is only about one-half of that of experiment, and so this model must be discounted.

We normalize the experimental data of Ref. [4] to the theoretical $E1$ curve (of Fig. 6) at 25 keV neutron energy where the ($M1$) contribution from the p-wave resonance at 255 keV is certain to be negligible. The fact that the theoretical cross section is very close to $1/v$ justifies our

TABLE V. Potential to reproduce the measured $J^\pi=2^-$ scattering cross section.

E (MeV)	σ_{fit} (b)	V_0 (MeV)	σ_{pot} (b)
0.0	1.60	−60.33	1.61
0.1	1.59	−60.58	1.58
0.2	1.51	−60.77	1.50
0.3	1.43	−60.96	1.43
0.4	1.35	−61.15	1.36
0.5	1.28	−61.33	1.29
0.6	1.21	−61.50	1.22

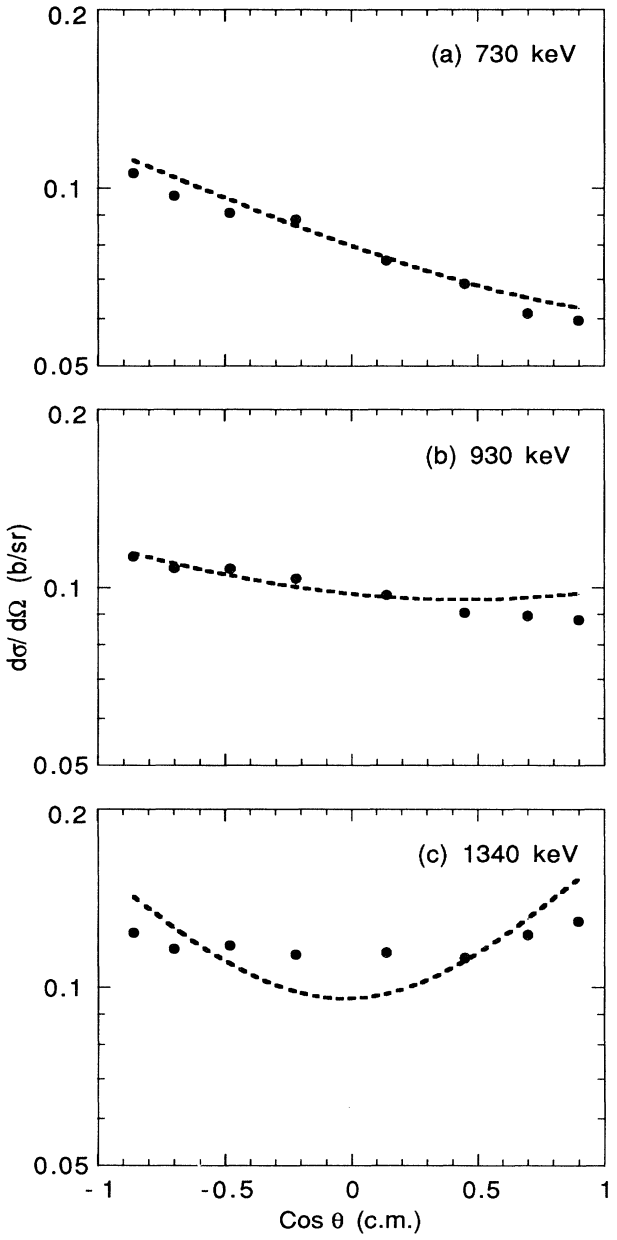

FIG. 5. Angular distribution of elastically scattered neutrons at different neutron energies. The data are from Ref. [22]. The respective curves employ the parameters of Table IV.

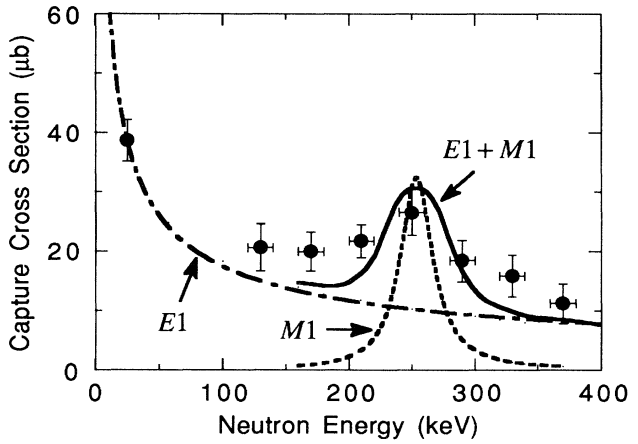

FIG. 6. Capture cross section in the resonance region of ^{7}Li. Circles are the data of Ref. [4] normalized to 39 μb at 25 keV. The curves are from the current calculations. The solid curve $E1+M1$ simulates the experimental resolution in an *approximate* way. The deviations between the data points and the solid curve are unimportant (cf. Fig. 4 of Ref. [4]); only the net area under the measured and calculated cross section curves are important for nucleosynthesis applications.

procedure and that of Ref. [4] in which the 25-keV monoenergetic cross section is deduced from the average cross section in a neutron spectrum that simulates a Maxwell-Boltzmann distribution and makes this energy a sound point to normalize data against theory. We then subtract this $E1$ component from the experimental data to yield the $M1$ resonance component.

V. RESONANCE MAGNETIC-DIPOLE CAPTURE

A. Valence-capture theory

The approach we use to estimate the $M1$ valence-capture width is exactly parallel to that of Ref. [23]. The essence of the theory is that a loosely bound nucleon orbiting in the potential field of an "inert" core of the residual nucleus makes a radiative transition to a lower orbit, the core remaining unchanged. In the simplest form of the theory and the one that is usually thought of as being the valence theory, the core is actually the ground state of the target nucleus. The initial (capture) state is projected onto the target $\otimes$ s.p. product, and the experimental measure of the squared amplitude of this projection is the reduced neutron width of the resonance state. Similarly, the measure of the projection of the final state onto the product of the target ground state and a (different) s.p. state is the spectroscopic factor determined in the (d,p) stripping reaction. In calculating the strength of the s.p. transition in this model, the initial s.p. wave function is treated as an $\mathcal{R}$-matrix state with a boundary condition appropriate to the actual resonance state and eigenvalue coinciding with it. The final bound s.p. state is treated as such; its eigenvalue coinciding with that of the actual final state. To obtain agreement between the s.p. eigenvalues and the experimental energies, the parameters of the potential well have to be varied (separately) somewhat from those of a global optical or real potential that would normally be used. This procedure can be defended on the grounds that the most important parts of the wave functions contributing to the radial component of the transition matrix element are, especially for the $E1$ case, those in the channel region of configuration space, and these are controlled by the state energies rather than by the internal details of the potential.

For the application of this model to $M1$ capture, the $E1$ operator $rY_{1,\mathcal{M}}$ (Eq. (13) of Ref. [23]) is replaced by the $M1$ operator

$$H'_{M1,\mathcal{M}}=\frac{e\hbar}{2mc}\left[\frac{3}{4\pi}\right]^{1/2}\left[\frac{\mu_I I_{\mathcal{M}}}{I}+\frac{\mu_n \sigma_{n,\mathcal{M}}}{\sigma}\right]. \tag{5}$$

Here e is the proton charge, m the nucleon mass, c the velocity of light, μ_I (μ_n) the magnetic moment (in units of nuclear magnetons μ_0) of the target nucleus (neutron), I the target-nucleus spin operator, and σ the Pauli spin operator for the neutron. From this expression the reduced matrix element for the spin factor can be computed, while the radial matrix element is simply the integral of the product of the initial-state radial wave function X_λ and the final-state radial wave function Φ_μ.

We use the reduced matrix element of the form

$$\frac{|\langle J_i\|H'_{M1,\mathcal{M}}\|J_f\rangle|^2}{2J_i+1}=\left[\frac{e\hbar}{2mc}\right]^2\frac{3}{4\pi}\mathcal{W}^{M1}. \tag{6}$$

Here J_i and J_f are the total angular momenta of the initial and final states, respectively. We assume, as part of the valence-capture theory, that these total angular momenta are constructed within the spin-orbit scheme; that is, the neutron spin and orbital angular momentum are coupled to give spin j, which is then coupled with target nucleus spin I to give the total spin J. With Eq. (5) and this convention, the expression for the ratio between the radiation and neutron widths of a s.p. state (defined within the constraints of $\mathcal{R}$-matrix theory and computed for a Woods-Saxon potential well adjusted to give its eigenvalue at the experimental resonance energy) is

$$\frac{\Gamma_{i(\gamma\to f)}}{2P_{\hat{l}}\gamma_i^2}=4k_\gamma^3\mathcal{W}^{M1}\left[\frac{e\hbar}{2mc}\right]^2\frac{1}{\hbar v}\times\left|\left[\frac{P_0}{P_l}\right]^{1/2}\left\langle\frac{u_i(r)}{u_i(a)}\middle|w_f(r)\right\rangle+\left\langle\frac{\mathcal{J}_l e^{i\varphi}+\mathcal{O}_l e^{-i\varphi}}{2}\middle|w_f(r)\right\rangle\right|^2, \tag{7}$$

where P_l is the penetration factor of neutron wave with orbital angular momentum l; k_γ is the photon wave number; v is the neutron velocity, u_i, w_f are the radial wave functions of the initial and final states; and $\mathcal{J}_l, \mathcal{O}_l$ are the incoming and outgoing wave combinations of the spherical Bessel and Neumann functions j_l and n_l:

$$\mathcal{O}_l(r)=-kr[n_l(kr)+ij_l(kr)] \tag{8}$$

and

$$\mathcal{O}_l(r)=-kr[n_l(kr)-ij_l(kr)]. \tag{9}$$

We can now use the s.p. estimate of the radiation width from Eq. (7) to obtain an expression for the compound-nucleus radiation width. Using the valence model assumption, the $\mathcal{R}$-matrix state describing the resonance can be expanded as

$$X_\lambda=c_{\lambda,i}u_i(r)+\cdots. \tag{10}$$

Hence the reduced neutron width is

$$\gamma_\lambda^2=(\hbar^2/2ma)c_{\lambda,i}^2u_i(a)^2. \tag{11}$$

With the final state expanded as

$$\phi_f(r)=\theta_f w_f(r)+\cdots, \tag{12}$$

the expression for the ratio of radiation and neutron width of the resonance state is given by

$$\Gamma_{\lambda(\gamma\to f)}/2P_l\gamma_\lambda^2=\theta_f^2\Gamma_{i(\gamma\to f)}/2P_l\gamma_i^2. \tag{13}$$

The $M1$ valence radiation width $\Gamma_{\lambda(\gamma\to f)}$ is obtained by multiplying the ratio calculated from the s.p. wave functions in a Woods-Saxon potential [see Eq. (7)] by the experimentally known quantities, namely, the spectroscopic factor of the final state θ_f^2 and the neutron width of the initial resonance state $2P_l\gamma_\lambda^2$.

B. Comparison to experiment

The normalized $M1$ resonance capture cross section is shown in Fig. 6. The circles indicate normalization of the data of Ref. [4] to 39 μb (the calculated $E1$ value) at 25 keV. After subtracting the $E1$ component, the net area of the capture cross section under the resonance is 2.2 ± 0.4 eV b. The area of the total cross section (see Fig. 2) is 0.865 MeV b. The ratio, in conjunction with the neutron width $\Gamma_n=40.6\pm0.6$ keV, gives the radiation width $\Gamma_\gamma=0.10\pm0.02$ eV. A similar analysis carried out by Imhof *et al.* [5] of their data yielded $\Gamma_\gamma=0.07\pm0.03$ eV. (By comparison, Wiescher, Steininger, and Käppeler [4] obtained $\Gamma_\gamma=0.026\pm0.008$ eV from the original data.) From our reanalyzed value and that of Ref. [5], we conclude that the $M1$ radiation width, which comprises only one transition (that to the ground state), is 0.09 eV with a possible uncertainty of 20%.

To compute the theoretical value of the valence radiation width, we assume that $1p_{3/2}$ states are the principal s.p. components of both the initial resonance and final (ground) state. With the magnetic moment of ^{7}Li equal to $3.256\mu_0$ and that of the neutron equal to $-1.913\mu_0$, the value of $\mathcal{W}^{M1}$ is computed to be 11.9. Combining this value with the computed radial overlap integral [in a Woods-Saxon potential ($R=2.5$ fm, $d=0.5$ fm) of depth 32.2 MeV to give the initial state at the resonance energy of 255 keV and of depth 38.8 MeV to give the binding energy (2.03 MeV) of the ground state], the radiation width is found to be $0.108\theta_f^2$ eV. With the value $\theta_f^2=0.87$ of Ref. [11], this expression gives $\Gamma_\gamma=0.094$ eV. This width agrees with the experimental width of 0.09 ± 0.02 eV and, hence, strongly supports the hypothesis that the valence-capture mechanism is the dominant process for radiative capture in the p-wave resonances of the ^{7}Li neutron-capture cross section. The computed $M1$ capture cross section corresponding to the theoretical value of the radiation width is shown in Fig. 6 superimposed on the $E1$ direct background cross section.

VI. CONCLUSIONS

We have made a complete analysis of the data that currently exist relating to the neutron-capture cross section of ^{7}Li up to 0.5 MeV. The thermal-neutron-capture cross section is consistent with the usual pattern of light nuclei in that it is quantitatively explainable by the direct- (potential-) capture theory for electric-dipole transitions. Agreement between the data and theory is well within the degree of uncertainty in the spectroscopic factors required for specifying the s.p. content of the final states. The branching ratio between the transition strengths to the ground- and first-excited states is described reasonably well by the theory.

The capture cross section at higher energy (25–100 keV) is of the right magnitude also to be of direct origin (or some collective variant thereof). Because only s waves are of significance over this energy range and the scattering cross sections do not change appreciably, it is very unlikely from a theoretical view that there is any significant departure of the capture cross section from the inverse neutron velocity ($1/v$) relationship. The capture cross sections calculated from the direct theory lie between the two sets of fast-neutron-capture data, but are considerably closer to the older data of Ref. [5] than to the more recent data of Ref. [4]. We see no reason on theoretical grounds for preferring the more recent data; therefore, we recommend that our theoretical curve consisting of the $E1$ direct-capture cross section plus $M1$ resonance capture with the adjusted theoretical radiation width $\Gamma_\gamma=0.094$ eV be used for astrophysical nucleosynthesis calculations until new experimental data [24] can be established. It follows that the conclusion of Ref. [4], that the ^{7}Li$(n,\gamma)^8$Li reaction is not the predominant link to the primordial r process for creating the heavier elements, is not supported.

One of the main objectives of this paper was to test the possible validity of the valence theory of neutron capture for $M1$ transitions. The data of Ref. [4] appear to offer an improved means for extracting the $M1$ radiative width for the transition from the p-wave $J=3$ resonance at 255 keV to the ground state of ^{8}Li. To extract this width we have carefully analyzed the total cross section and scattered neutron angular-distribution data to establish the s-wave neutron-scattering lengths through the resonance region. From this we can calculate the underlying $E1$ capture cross section to be subtracted from the data of Ref. [4] (renormalized to the theory at 25 keV) to yield the resonance-capture cross section. The radiation width extracted in this way is in good agreement with the value calculated from the valence theory. It thus appears that $M1$ valence capture may be a very significant capture mechanism, even though the factor that makes it so easily estimable in the $E1$ case—namely, the radial dependence of the $E1$ operator pushing the important regions of the wave functions into the channel space—is not significant here.

ACKNOWLEDGMENTS

We thank C. H. Johnson, M. J. Martin, R. O. Lane, and R. W. Sharpe for helpful comments. The current research was sponsored by the U.S. Department of Energy under Contract No. W-7405-eng-36 with the University of California (Los Alamos) and Contract No. DE-AC05-84OR21400 with Martin Marietta Energy Systems, Inc. (Oak Ridge).

[1] A. M. Lane and J. E. Lynn, Nucl. Phys. **17**, 563 (1960); **17**, 586 (1960).
[2] S. Raman, R. F. Carlton, J. C. Wells, E. T. Jurney, and J. E. Lynn, Phys. Rev. C **32**, 18 (1985).
[3] R. A. Malaney and W. A. Fowler, in *The Origin and Distribution of the Elements*, edited by G. J. Mathews (World Scientific, Singapore, 1987), p. 76.
[4] M. Wiescher, R. Steininger, and F. Käppeler, Astrophys. J. **344**, 464 (1989).
[5] W. L. Imhof, R. G. Johnson, F. J. Vaughn, and M. Walt,

Phys. Rev. **114**, 1037 (1959).
[6] P. E. Hodgson, Rep. Prog. Phys. **47**, 613 (1984).
[7] C. Mahaux and R. Sartor, Nucl. Phys. **A468**, 193 (1987); Phys. Rev. C **36**, 1777 (1987).
[8] Thermal capture results presented here are substantially the same as those appearing (as a private communication) in the compilation by F. Ajzenberg-Selove and T. Lauritsen [Nucl. Phys. **A227**, 1 (1974)]. These results are formalized here in view of their importance.
[9] See references in S. F. Mughabghab and D. I. Garber, Brookhaven National Laboratory Report BNL-325, 1971, p. 1–2.
[10] L. Koester, K. Knopf, and W. Waschkowski, Z. Phys. A **312**, 81 (1983).
[11] J. P. Schiffer, G. C. Morrison, R. H. Siemssen, and B. Zeidman, Phys. Rev. **164**, 1274 (1967).
[12] J. E. Lynn, S. Kahane, and S. Raman, Phys. Rev. C **35**, 26 (1987).
[13] S. Kahane, J. E. Lynn, and S. Raman, Phys. Rev. C **36**, 533 (1987).
[14] S. Raman, S. Kahane, R. M. Moon, J. A. Fernandez-Baca, J. L. Zarestky, J. E. Lynn, and J. W. Richardson, Phys. Rev. C **39**, 1297 (1989).
[15] S. Raman, S. Kahane, and J. E. Lynn, in *Proceedings of the International Conference on Nuclear Data for Science and Technology, Mito, Japan,* edited by S. Igarasi (Saikon, Tokyo, 1988), p. 645.
[16] E. P. Wigner and L. Eisenbud, Phys. Rev. **72**, 29 (1947).
[17] A. M. Lane and R. G. Thomas, Rev. Mod. Phys. **30**, 257 (1958).
[18] H. D. Knox and R. O. Lane, Nucl. Phys. **A359**, 131 (1981).
[19] H. D. Knox, D. A. Resler, and R. O. Lane, Nucl. Phys. **A466**, 245 (1987).
[20] See data and references in V. McLane, C. L. Dunford, and P. F. Rose, *Neutron Cross Sections* (Academic, San Diego, 1988), Vol. 2, p. 14.
[21] K. W. McVoy, Phys. Lett. **17**, 42 (1965).
[22] R. O. Lane, A. S. Langsdorf, Jr., J. E. Monahan, and A. J. Elwyn, Ann. Phys. (N.Y.) **12**, 135 (1961). See also D. I. Garber, L. G. Strömberg, M. D. Goldberg, D. E. Cullen, and V. C. May, Brookhaven National Laboratory Report BNL 400, 1970, p. 3-7-7.
[23] S. Raman, M. Igashira, Y. Dozono, H. Kitazawa, M. Mizumoto, and J. E. Lynn, Phys. Rev. C **41**, 458 (1990).
[24] Measurements [detection of prompt γ rays from the ^{7}Li$(n,\gamma)^8$Li reaction with a NaI(Tl) detector] are now in progress at the Tokyo Institute of Technology and preliminary indications are that the capture cross section at 30 keV is indeed about 2 times larger than the value reported in Ref. [4] [Y. Nagai (private communication)].